

Super-diffusive transport in two-dimensional Fermionic wires

Junaid Majeed Bhat

*Department of Physics, Faculty of Mathematics and Physics,
University of Ljubljana, 1000 Ljubljana, Slovenia*

(Dated: July 8, 2024)

We present a two-dimensional model of a Fermionic wire which shows a power-law conductance behavior despite the presence of uncorrelated disorder along the direction of the transport. The power-law behavior is attributed to the presence of energy eigenstates of diverging localization length below some energy cutoff, E_c . To study transport, we place the wire in contact with electron reservoirs biased around a Fermi level, E . We show that the conductance scales super-diffusively for $|E| < E_c$ and decays exponentially for $|E| > E_c$. At $|E| = E_c$, we show that the conductance scales diffusively or with different sub-diffusive power-laws depending on the sign of the expectation value of the disorder and the parameters of the wire.

Introduction of disorder in quadratic systems is known to generically cause localization since the seminal work of Anderson¹ and other subsequent works²⁻⁵. Thus, the conductance decays exponentially with the system size in disordered systems. On the other hand, the conductance in disorder free quadratic systems is ballistic. While these behaviors of the conductance are the two extremes of perfectly conducting and insulating behaviors, respectively, conductance can also scale as a power-law ($1/N^\alpha$) with the system size, N . The scaling can be categorized into diffusive ($\alpha = 1$), super-diffusive ($\alpha < 1$) and sub-diffusive ($\alpha > 1$) behaviors. Diffusive scaling is in general expected on addition of interactions to quadratic systems⁶. Super-diffusive and sub-diffusive are therefore considered anomalous. Sub-diffusive transport has been observed in disordered interacting spin systems⁷⁻¹⁰ and also at the band edges of quadratic Fermionic systems¹¹⁻¹³. Super-diffusive transport is observed in quadratic systems by introducing certain types of correlated^{14,15} or aperiodic¹⁶ disorders. Recent studies have shown super-diffusive transport in interacting spin systems¹⁷⁻¹⁹ and also in certain type of dephasing models²⁰.

The phenomenon of Anderson localization also occurs in classical systems of harmonic wires²¹⁻²³. Nevertheless, certain peculiar systems are known to show power-law scaling of energy current even in the presence of uncorrelated disorder²⁴⁻²⁶. A simple example is a 1D harmonic wire with disordered masses first studied in detail by Casher and Lebowitz²⁴. In this case, the localization length of the normal modes of the wire diverges as the conducting frequency approaches zero²¹. Therefore, low frequency modes contribute to the transport effectively giving rise to a power-law scaling of the energy current. The exact scaling is determined by the behavior of the localization length as the frequency, $\omega \rightarrow 0$ and the low-frequency behavior of the heat transmission²⁶⁻³¹.

To our knowledge, such peculiar models have not been discussed in the context of Fermionic wires. In this work, we introduce a simple 2D model for Fermionic wires that realizes physics analogous to 1D mass disordered harmonic wires. Therefore, our model shows a power-law

scaling of the conductance in presence of uncorrelated disorder along the direction of the transport. This is in contrast with the earlier studies of 1D Fermionic wires where the disorder is either correlated^{14,15} or aperiodic¹⁶. While in the harmonic wires the localization length diverges only at a particular point in the energy spectrum, our 2D model contains eigenfunctions of diverging localization lengths at energies with absolute values less than some cut off, E_c . Therefore, E_c effectively behaves as a mobility edge.

To study electron transport, we consider a sample of the wire of size $L \times W$ and place it in contact with metallic leads along its vertically opposite edges. We then employ the non-equilibrium Green's function formalism (NEGF), to look at the scaling of the conductance with L while the leads are biased around a Fermi-level, E . We find that for $|E| < E_c$, the conductance shows a super-diffusive behavior and for $|E| > E_c$ the conductance scales exponentially with the length of the wire. At the transition point $|E| = E_c$, the conductance scales with different power-laws for positive, negative or zero expectation value of the disorder. We present heuristic arguments that explain all the numerically observed power-laws. However, the underlying assumption of these arguments fails for the cases where $|E| = E_c$, and the expectation value of disorder vanishes. In these cases, the observed power-laws are underestimated by a factor of L by the theoretical arguments, opening up an interesting problem for further studies.

This paper is structured as follows: In Sec. (I), we lay down the details of the wire, leads, and the contacts between them. We also discuss the eigenfunctions of the isolated wire and illustrate why we expect diverging localization lengths for certain range of energies. In Sec. (II), we set up the NEGF formalism which we use to look at the average behavior of the conductance. We then consider the Lyapunov exponents, inverse of the localization length, in Sec. (III) for the wave-functions of the wire and present results for its asymptotic behavior around the point where it vanishes. In the penultimate section, Sec. (IV), we use the NEGF expression for the conductance and the knowledge of the Lyapunov exponents to

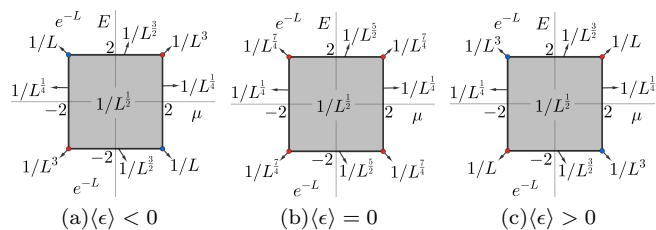


FIG. 1. Power laws for the behavior of the conductance at different Fermi Levels and the parameter μ .

determine the different power-laws for the conductance and also present numerical results for its behavior. We conclude in Sec. (V).

I. THE MODEL

We consider the wire Hamiltonian, \mathcal{H}_W , to be given by a tight-binding model defined on a rectangular lattice of size $L \times W$. Let us label the annihilation and creation operators, satisfying usual anti-commutation relations, at a site (x, y) as $(\psi(x, y), \psi^\dagger(x, y))$ on the wire. The Hamiltonian of the wire is then given by,

$$\mathcal{H}_W = \sum_{x=1}^L \epsilon_x \Psi^\dagger(x) H_0 \Psi(x) + \sum_{x=1}^{L-1} [\Psi^\dagger(x) \Psi(x+1) + \text{h.c.}], \quad (1)$$

where, $\Psi(x) = (\psi(x, 1), \psi(x, 2), \dots, \psi(x, W))^T$. ϵ_x is the disorder parameter chosen randomly at every x with expectation value of $\langle \epsilon \rangle$.

The eigenstates of the wire are given by, $\psi_{E_{k_m}}(x, y) = \chi_k(y) \phi_{k,m}(x)$, where $k = 1, 2, \dots, W$ and $m = 1, 2, 3, \dots, L$. χ_k is an eigenvector of H_0 with eigenvalue λ_k and $\phi_{k,m}(x)$ satisfy,

$$\phi_{k,m}(x-1) + \lambda_k \epsilon_x \phi_{k,m}(x) + \phi_{k,m}(x+1) = E_{k,m} \phi_{k,m}(x). \quad (2)$$

The solutions for $\phi_{k,m}(x)$ correspond to the wavefunctions of a 1D Anderson insulator of length L with onsite disorder of effective strength proportional to λ_k . Therefore, the localization length of the eigenvectors depends on λ_k and diverges if λ_k vanishes. Thus, if λ_k 's are banded and cross the value zero, then in the limit $W \rightarrow \infty$ there are extended eigenstates with energies of absolute value less than $E_c = 2$. So, a fraction of the eigenfunctions of the wire which correspond to λ_k near zero contribute to the transport giving rise to a power-law scaling of the conductance. This power-law is determined by the behavior of the localization length near $\lambda_k = 0$, which we discuss later. While this physics holds for any choice of H_0 , we now fix, for the rest of the paper, a simple choice of H_0 corresponding to nearest neighbor hopping with an onsite chemical potential of μ , so that its spectrum is given by $\lambda_k = \mu + 2 \cos \frac{k\pi}{W+1}$.

To probe the electron transport across the wire, we place it in contact with metallic leads acting as electron reservoirs at its two opposite edges along y -direction. We then use the NEGF formalism to study the conductance with the reservoirs kept at zero temperatures and biased around a Fermi-level, E . The two reservoirs are themselves modeled as nearest-neighbor tight-binding Hamiltonians on a square lattice with hoppings along x and y directions given by η_{bx} and η_{by} , respectively. The contacts are also modeled as tight-binding Hamiltonians with hopping strength η_c . For details of the reservoir and contact Hamiltonians see Appendix A.

We obtain different behaviors of the conductance with respect to E and μ that are summarized in Fig. (1). Inside the shaded square and along its vertical edges in Fig. (1), we see a super-diffusive scaling of the conductance. Along the horizontal edges of the square and at the corners the conductance scales sub-diffusively except for some cases where it scales diffusively, and shows an interesting dependence on the sign of the expectation value of the disorder. Outside the shaded square, the conductance scales as e^{-L} . The behavior of the conductance is determined by the behavior of electron transmission at the Fermi level E and the localization length near $\lambda_k = 0$. So, let us discuss the two separately.

II. NEGF CONDUCTANCE

The non-equilibrium steady state (NESS) of the wire can be obtained using the NEGF formalism in terms of the effective non-equilibrium Green's function for the wire defined as^{32,33}, $G^+(E) = (E - H_W - \Sigma_L(E) - \Sigma_R(E))^{-1}$, where $\Sigma_L(E)$ and $\Sigma_R(E)$ are the self energy contributions due to the reservoirs, and H_W is the full hopping matrix of the wire. For the reservoirs kept at zero temperatures and their chemical potential biased around a Fermi-level E , the conductance of the wire, in units of $e^2/h = 1$, is given in terms of $G^+(E)$ as, $T(E) = 4\pi^2 \text{Tr}[G^+(E)\Gamma_R(E)G^-(E)\Gamma_L(E)]$, where $G^-(E) = [G^+(E)]^\dagger$ and $\Gamma_{L/R} = (\Sigma_{L/R}^\dagger - \Sigma_{L/R})/(2\pi i)$.

While the above formula holds for arbitrary lattice models, for our model this could be approximated by

$$\tau(E) = \frac{T(E)}{W} \approx \frac{4}{\pi} \int_0^\pi d\mathbf{k} |F_L(\lambda_{\mathbf{k}})|^2, \quad (3)$$

where $F_L(\lambda_{\mathbf{k}}) = \gamma^2/[p_L(\lambda_{\mathbf{k}}) + i\gamma[p_{L-1}(\lambda_{\mathbf{k}}) + q_L(\lambda_{\mathbf{k}})] - \gamma^2 q_{L-1}(\lambda_{\mathbf{k}})]$ and $\gamma = \frac{\eta_c^2}{\eta_{bx}}$, in the limit $W \rightarrow \infty$ and $|\eta_{bx}| \gg |E| + |2\eta_{by}|$, see Appendix B. The integral runs over the spectrum of H_0 in the limit $W \rightarrow \infty$, given by $\mu + 2 \cos(\mathbf{k})$, $\mathbf{k} \in (0, \pi)$. $p_L(\lambda_{\mathbf{k}})$ and $q_L(\lambda_{\mathbf{k}})$ are obtained via same iteration equations, which for $p_L(\lambda_{\mathbf{k}})$ reads $p_{i+1}(\lambda_{\mathbf{k}}) = (-E + \epsilon_{i+1}\lambda_{\mathbf{k}})p_i(\lambda_{\mathbf{k}}) - p_{i-1}(\lambda_{\mathbf{k}})$, but with different initial conditions. Therefore, it suffices to consider only one of the two. It is clear that the asymptotic behavior of the $p_L(\lambda_{\mathbf{k}})$ with L eventually controls the behavior of the conductance with L . Also, note that

the iteration equation for $p_i(\lambda_{\mathbf{k}})$ is the same as the equation for $\phi_{k,m}(i)$. Therefore, the asymptotic behavior of $p_L(\lambda_{\mathbf{k}})$ also gives the localization length of the eigenvec-

tors of the wire. We now discuss the behavior of $p_L(\lambda_{\mathbf{k}})$ as $\lambda_{\mathbf{k}} \rightarrow 0$, which we later use to determine the scaling of the conductance.

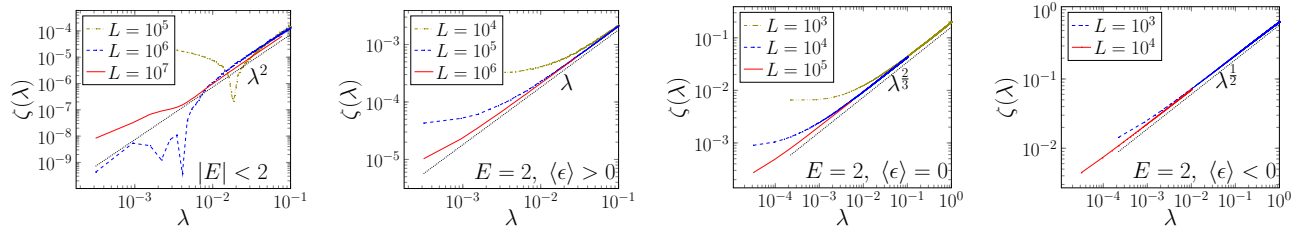


FIG. 2. Lyapunov exponents for the iteration equation, Eq. (4) for $|E| < 2$ and $E = 2$ with positive, negative and zero expectation value of the disorder. For $E = -2$, $\zeta(\lambda) \sim \lambda$ for $\langle \epsilon \rangle < 0$ and $\zeta(\lambda) \sim \lambda^{1/2}$ for $\langle \epsilon \rangle > 0$. The data presented is averaged over 10^3 realizations of the disorder chosen uniformly from the intervals $(-1, 0)$, $(-1, 1)$ and $(0, 1)$ for negative, zero and positive expectation value cases, respectively.

III. LYAPUNOV EXPONENTS

Let us consider the iteration equation for $p_L(\lambda)$, we have

$$p_{i+1}(\lambda) = (-E + \epsilon_{i+1}\lambda)p_i(\lambda) - p_{i-1}(\lambda). \quad (4)$$

We have dropped the \mathbf{k} subscript on λ for now, and we will only consider $\lambda > 0$, as $\lambda < 0$ is equivalent to shifting the sign of the disorder parameter. A theorem due to Furstenberg³⁴, guarantees non-negativity and the existence of the Lyapunov exponent, inverse of the localization length, defined as,

$$\zeta(\lambda) = \lim_{L \rightarrow \infty} \frac{1}{L} \langle \log |p_L(\lambda)| \rangle, \quad (5)$$

for any initial condition, and therefore $p_L(\lambda) \sim e^{L\zeta(\lambda)}$.

For $|E| \leq 2$, $\zeta(\lambda) \rightarrow 0$ as $\lambda \rightarrow 0$. Therefore, near zero λ values such that $L\zeta(\lambda) < 1$, contribute in Eq. (3). Thus, the behavior of $\zeta(\lambda)$ near $\lambda = 0$ is crucial to the scaling of the conductance. We present numerical results on this behavior at different E in Fig. (2). We see that while for $|E| < 2$, $\zeta(\lambda) \sim \lambda^2$ irrespective of the expectation value of the disorder, for $|E| = 2$ the behavior of $\zeta(\lambda)$ is different for different signs of the expectation value of the disorder. For $E = 2$, we find $\zeta(\lambda) \sim \lambda$, $\zeta(\lambda) \sim \lambda^{2/3}$, and $\zeta(\lambda) \sim \lambda^{1/2}$ for positive, zero and negative expectation value of the disorder, respectively. For $E = -2$, the behaviors are the same as $E = 2$ except that $\zeta(\lambda) \sim \lambda^{1/2}$ for positive expectation value and $\zeta(\lambda) \sim \lambda$ for negative expectation value of the disorder.

We outline the proof here and present the details in the Appendix C. Let us consider the case of $|E| < 2$. We follow the steps of Matsuda and Ishii in Ref. 21 as they considered the iteration equation, Eq. (4), for $E = -2$ and $\langle \epsilon \rangle < 0$ in the context of classical harmonic wires with mass disorder. We start by making the change of

variables,

$$\frac{p_{n+1}(\lambda)}{p_n(\lambda)} = \frac{\cos(\theta_n + h(\lambda, E))}{\cos \theta_n}, \quad (6)$$

where $2 \cos h(\lambda, E) = -E + \langle \epsilon \rangle \lambda$ so that the iteration equation now becomes,

$$\theta_{n+1} = \arctan \left[\tan(\theta_n + h(\lambda, E)) + \frac{\lambda(\epsilon - \langle \epsilon \rangle)}{\sin h(\lambda, E)} \right] = \bar{\Theta}[\theta_n, \lambda]. \quad (7)$$

The Lyapunov exponent in terms of the variable θ , is given by

$$\zeta(\lambda) = \lim_{L \rightarrow \infty} \frac{1}{L} \left\langle \sum_{n=1}^L \log \left| \frac{\cos(\theta_n + h(\lambda, E))}{\cos \theta_n} \right| \right\rangle, \quad (8)$$

$$= \int_{-\pi/2}^{\pi/2} d\theta \mathbf{P}[\theta, \lambda] \log \left| \frac{\cos(\theta + h(\lambda, E))}{\cos \theta} \right|. \quad (9)$$

In the last step we have replaced the average over "time" in the Marko process defined by the iteration equation, Eq. (4), by the integral over the invariant distribution $\mathbf{P}[\theta, \lambda]$ of the Marko process in accordance with the ergodic hypothesis. Expanding Eq. (9) in orders of λ we have,

$$\zeta(\lambda) = \int_{-\pi/2}^{\pi/2} d\theta \log |\cos \theta| \left[\zeta_0(\theta, E) + \lambda \zeta_1(\theta, E) + \lambda^2 \zeta_2(\theta, E) + \mathcal{O}(\lambda^3) \right]. \quad (10)$$

Assuming $h(\lambda, E) = \sum_{i=0}^{\infty} h_i(E)\lambda^i$ and $\mathbf{P}[\theta, \lambda] = \sum_{i=0}^{\infty} \mathbf{P}_i(\theta)\lambda^i$, the coefficients $\zeta_i(\theta, E)$ depend on θ and E via the functions $\mathbf{P}_i(\theta)$ and $h_i(E)$. Therefore, we need to determine $\mathbf{P}[\theta, \lambda]$ at least up to order λ^2 to find $\zeta(\lambda)$. It can be shown that the invariant distribution satisfies the self-consistent equation,

$$\mathbf{P}[\theta, \lambda] - \int d\epsilon \mathbf{P}[\bar{\Theta}[\theta, \lambda], \lambda] \partial_{\theta} \bar{\Theta}[\theta, \lambda] \mathbf{p}(\epsilon) = 0, \quad (11)$$

where $\mathbf{p}(\epsilon_x)$ is the probability distribution for ϵ_x and

$$\Theta[\theta, \lambda] = \arctan \left[\tan \theta - \frac{\lambda(\epsilon - \langle \epsilon \rangle)}{\sin h(\lambda, E)} \right] - h(\lambda, E), \quad (12)$$

is the inverse of the function $\bar{\Theta}[\theta, \lambda]$. Expanding the L.H.S of Eq. (11) in orders of λ and setting each order to

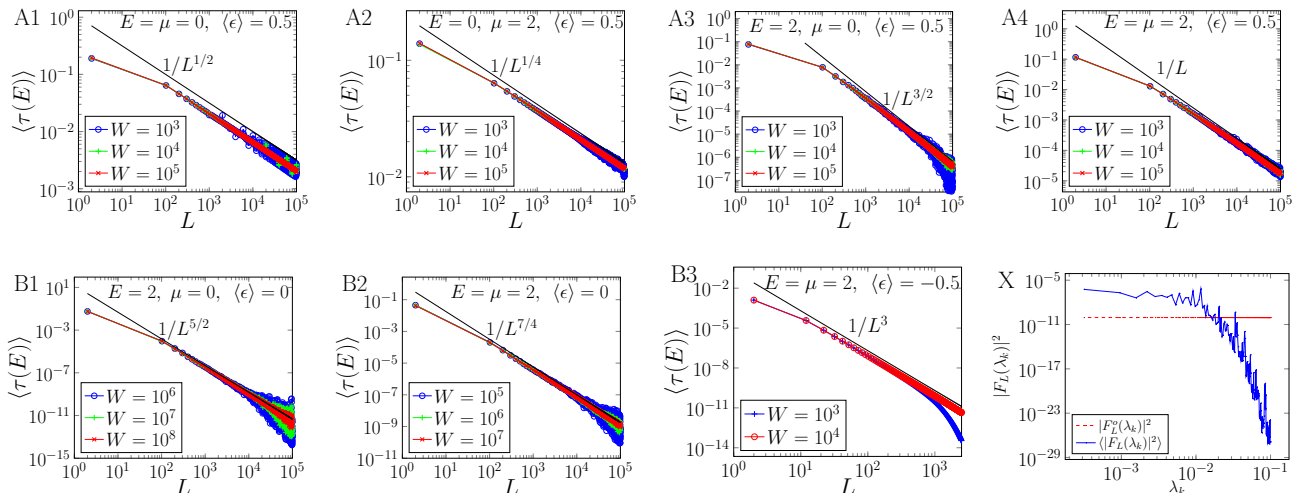


FIG. 3. Numerically observed power-laws for different Fermi levels and the parameter, μ . We see a good agreement with the predicted values as the width of the wire is increased except for the cases B1 and B2. For these two cases the theoretical arguments predict $1/L^{7/2}$ and $1/L^{11/4}$, respectively. The theoretical arguments predict slower transport as these arguments underestimate $\langle |F_L(\lambda_{\mathbf{k}})|^2 \rangle$ as can be seen from panel X. The data presented is averaged over 10^3 disorder realizations. Parameter values for X, $W = 10L = 10^4$, $E = 2$, $\mu = 0$ and $\langle \epsilon \rangle = 0$.

The proof relies on the fact that $\theta \in (-\pi/2, \pi/2)$ is bounded which is true as long as $h(\lambda, E)$ is real or equivalently $|-E + \langle \epsilon \rangle \lambda| < 2$. Therefore, considering only $\lambda > 0$, it also works for the cases where $E = -2$, $\langle \epsilon \rangle < 0$ and $E = 2$, $\langle \epsilon \rangle > 0$. However, when $|E| = 2$, the expansion for $h(\lambda, E)$ is different as it now has half integer powers of λ also. This makes the leading contribution to the Lyapunov exponent, $\zeta(\lambda) \sim \lambda$ for the two cases.

For $|-E + \langle \epsilon \rangle \lambda| \geq 2$, the above proof does not work. The cases where this happens are $|E| = 2$ with $\langle \epsilon \rangle = 0$, $E = 2$ with $\langle \epsilon \rangle < 0$, and $E = -2$ with $\langle \epsilon \rangle < 0$. Let us first consider the latter two cases. For these cases the Lyapunov exponent is finite even if the disorder is replaced by its average, $\langle \epsilon \rangle$. In that case, the solution for Eq. (4) is given by $p_L(\lambda) = \frac{\sin(L+1)h(\lambda)}{\sin h(\lambda)}$. Therefore,

in the limit $L \rightarrow \infty$, $p_L(\lambda) \sim e^{\sqrt{\langle \epsilon \rangle \lambda L}$ which gives $\zeta(\lambda) \sim \lambda^{1/2}$. The disorder only contributes at higher orders in λ . The case where $\langle \epsilon \rangle = 0$ is very subtle and requires an elaborate proof. We point the reader to Ref. 26 which considers Eq. (4) for $E = -2$ in the context of harmonic wires with disordered magnetic fields. In this work, the Lyapunov exponents are determined by mapping Eq. (4) for $E = -2$ to a harmonic oscillator with noisy frequency

zero gives, $\zeta_0(\theta, E) = 0$, $\zeta_1(\theta, E) = 0$, and $\zeta_2(\theta, E) \neq 0$ for the zeroth, first and second order in λ , respectively. Hence, the zeroth order and the first order terms vanish in the expansion of $\zeta(\lambda)$ and therefore $\zeta(\lambda) \sim \lambda^2$ as $\lambda \rightarrow 0$.

which is well studied in literature³⁵. It is shown that $\zeta(\lambda) \sim \lambda^{2/3}$ for $\langle \epsilon \rangle = 0$, and also $\zeta(\lambda) \sim \lambda^{1/2}$ and $\zeta(\lambda) \sim \lambda$ for $\langle \epsilon \rangle > 0$ and $\langle \epsilon \rangle < 0$, respectively.

IV. SCALING OF THE CONDUCTANCE

We now determine the scaling of the average behavior of the conductance. Let us assume $\zeta(\lambda_{\mathbf{k}}) \sim |\lambda_{\mathbf{k}}|^a$, where a is known from our previous results. Therefore, the $|\lambda_{\mathbf{k}}|$ values for which $|\lambda_{\mathbf{k}}|^a L < 1$ contribute in the integral for the conductance in Eq. (3). Hence, in the limit $L \rightarrow \infty$, we can cutoff the integral over \mathbf{k} as follows,

$$\langle \tau(E) \rangle \approx \frac{4}{\pi} \lim_{L \rightarrow \infty} \int_{\mathbf{k}_* - \mathbf{k}_c}^{\mathbf{k}_* + \mathbf{k}_c} d\mathbf{k} \langle |F_L(\lambda_{\mathbf{k}})|^2 \rangle, \quad (13)$$

where \mathbf{k}_* is the point such that $\lambda_{\mathbf{k}_*} = 0$, and $\mathbf{k}_c > 0$ is a small deviation from \mathbf{k}_* such that $|\lambda_{\mathbf{k}_* + \mathbf{k}_c}|^a L \sim 1$. Let the Taylor expansion of $\lambda_{\mathbf{k}}$ around $\mathbf{k} = \mathbf{k}_*$ be $\lambda_{\mathbf{k}_* + \mathbf{k}_c} = \lambda_0 \mathbf{k}_c^b + \mathcal{O}(\mathbf{k}_c^{b+1})$, we have $\mathbf{k}_c \sim 1/L^{1/(ab)}$.

Within the range of integration in Eq. (13), the disorder is effectively absent so we make an assumption by replacing $\langle |F_L(\lambda_{\mathbf{k}})|^2 \rangle$ by $|F_L^o(\lambda_{\mathbf{k}})|^2$ which is same quantity computed with the disorder replaced by its average

at every x . With some simple algebra we can show,

$$F_L^o(\lambda_{\mathbf{k}}) = \frac{\gamma \sin q_{\mathbf{k}}}{\sin q_{\mathbf{k}}(L+1) + 2i\gamma \sin q_{\mathbf{k}}L - \gamma^2 \sin q_{\mathbf{k}}(L-1)}. \quad (14)$$

where $q_{\mathbf{k}} = \arccos[(-E + \lambda_{\mathbf{k}} \langle \epsilon \rangle)/2]$. Using this assumption Eq. (13) reduces to,

$$\langle \tau(E) \rangle \approx \frac{4}{\pi} \lim_{L \rightarrow \infty} \int_{\mathbf{k}_* - \mathbf{k}_c}^{\mathbf{k}_* + \mathbf{k}_c} d\mathbf{k} |F_L^o(\lambda_{\mathbf{k}})|^2. \quad (15)$$

For $|E| < 2$, the integrand in Eq. (15) is finite at $\mathbf{k} = \mathbf{k}_*$ and is highly oscillatory with L around \mathbf{k}_* . However, as $L \rightarrow \infty$, it approximately averages out to, $|\bar{F}^o(q_{\mathbf{k}})|^2 \approx \left| \frac{\gamma}{2(1+\gamma^2)} \sin q_{\mathbf{k}} \right|^2$, under the integral sign (see Appendix D). Using $\bar{F}^o(q_{\mathbf{k}})$ in Eq. (15), we get $\langle \tau(E) \rangle \sim 1/L^{ab}$. Now, $a = 2$ for all values of $|\mu| \leq 2$ but $b = 1$ for $|\mu| < 2$ and $b = 2$ for $|\mu| = 2$. Therefore, we expect $1/L^{1/2}$ and $1/L^{1/4}$ for these two cases, respectively, and the numerical results shown in panels A1 and A2 of Fig. (3) are in good agreement. For $|E| > 2$ or $|\mu| > 2$ the integrand decays exponentially so does the conductance.

For $|E| = 2$ the integrand requires a bit more attention as $q_{\mathbf{k}_*} = \pi$ which means $F_L^o(\lambda_{\mathbf{k}_*})$ vanishes. Therefore, its behavior around \mathbf{k}_* matters in the scaling of the conductance. This behavior around \mathbf{k}_* is different for real and imaginary $q_{\mathbf{k}}$. Let us first consider $q_{\mathbf{k}}$ to be real, then from Eq. (14), $F_L^o(\lambda_{\mathbf{k}})$ is highly oscillatory with L and once again averages out to $\bar{F}^o(q_{\mathbf{k}}) \sim |\bar{\mathbf{k}}|^{b/2}$, $\bar{\mathbf{k}} = \mathbf{k} - \mathbf{k}_*$. Using this in Eq. (15) we have, $\langle \tau(E) \rangle \sim \int_0^{L^{1/(ab)}} d\bar{\mathbf{k}} \bar{\mathbf{k}}^{b/2} = 1/L^{\frac{b+2}{2ab}}$. This power-law is valid only if $q_{\mathbf{k}}$ is real, equivalently $|-E + \lambda_0 \langle \epsilon \rangle \bar{\mathbf{k}}^b| < 2$, within the range of the integration. Therefore, the sign of the term $\lambda_0 \langle \epsilon \rangle \bar{\mathbf{k}}^b$ is important as $|E| = 2$. Depending on sign of $\langle \epsilon \rangle$ and the corresponding values of b and a , we find several different cases. These cases have E, μ values which correspond to $1/L$ marked corners of the shaded square and its horizontal edges in Fig.(1a) for $\langle \epsilon \rangle < 0$ as well as in Fig.(1c) for $\langle \epsilon \rangle > 0$. At those corners $b = 2$, $a = 1$ giving a diffusive scaling $\langle \tau(E) \rangle \sim 1/L$, and at the horizontal edges $b = 1$, $a = 1$ giving $\langle \tau(E) \rangle \sim 1/L^{3/2}$, respectively. We show a comparison between numerical computations and the predicted power-laws in panels A3, A4 of Fig. (3) and once again we see a good agreement.

Let us now consider $q_{\mathbf{k}}$ to be imaginary which means $|-E + \lambda_0 \langle \epsilon \rangle \bar{\mathbf{k}}^b| \geq 2$. This happens for the cases which correspond to the horizontal edges (B1) and the corners (B2) of Fig. (1b) for $\langle \epsilon \rangle = 0$ and to the $1/L^3$ marked corners (B3) of Fig. (1a) and Fig. (1c). For B1 and B2, $\langle \epsilon \rangle = 0$ and therefore, $\lim_{L \rightarrow \infty} \lim_{q_{\mathbf{k}_*} \rightarrow \pi} F_L^o(\lambda_{\mathbf{k}}) \sim 1/L$. For the case B3, $\langle \epsilon \rangle \neq 0$ but $\mathbf{k}_c \sim \frac{1}{L}$ as $a = 1/2$ and $b = 2$, and once again $\lim_{L \rightarrow \infty} \lim_{q_{\mathbf{k}_*} \rightarrow \pi} F_L^o(\lambda_{\mathbf{k}}) \sim 1/L^{12,13}$. Using this behavior of $F_L^o(\lambda_{\mathbf{k}})$ and the corresponding values of a and b , we get $1/L^{7/2}$, $1/L^{11/4}$ and $1/L^3$ for B1, B2 and B3, respectively.

Panels B1, B2 and B3 in Fig. (3) show a comparison with the numerically calculated conductance for these

cases. We see that the theoretical arguments underestimate the power-law approximately by a factor of L for B1 and B2. While the theory predicts $1/L^{7/2}$ and $1/L^{11/4}$ for the two cases, numerical data agrees with $1/L^{5/2}$ and $1/L^{7/4}$, respectively. The reason being that the approximation that $|F_L^o(\lambda_{\mathbf{k}})|^2 = \langle |F_L(\lambda_{\mathbf{k}})|^2 \rangle$ for $\lambda_{\mathbf{k}} \rightarrow 0$ fails, and in fact it underestimates $\langle |F_L(\lambda_{\mathbf{k}})|^2 \rangle$. This can be seen in panel X of Fig. (3) where we plot a comparison between $|F_L^o(\lambda_{\mathbf{k}})|^2$ and $\langle |F_L(\lambda_{\mathbf{k}})|^2 \rangle$ for the parameter values corresponding to the case B1. It is not clear how to estimate $\langle |F_L(\lambda_{\mathbf{k}})|^2 \rangle$ and predict the observed power-laws for these two cases, and therefore our work opens up an interesting question for further studies. A similar issue has also been pointed out for harmonic wires in presence of disordered magnetic fields²⁶. For the case B3, we see a perfect agreement between the theory and the numerical computations.

V. CONCLUSIONS

In conclusion, we looked at a model of a disordered Fermionic wire in two-dimensions and studied the scaling of conductance with the length of the wire along the direction of transport. In particular, we find that despite the presence of uncorrelated disorder along the direction of the transport, the conductance shows a super-diffusive scaling. This is attributed to the presence of eigenstates with diverging localization lengths at energies with absolute values less than a cutoff E_c . Using heuristic arguments, we determined the super-diffusive behavior to be $1/L^{1/2}$ which agrees with the numerical computations. We also showed that at $|E| = E_c$ and at some special values of the parameters of the wire the conductance shows various sub-diffusive scalings and also diffusive scaling. The sub-diffusive power-laws are sensitive to the the sign of the expectation value of the disorder and are also different if the expectation value of the disorder vanishes.

Our heuristic arguments predict the different power-laws at $|E| = E_c$ except when the disorder average vanishes. For this case, the assumptions underlying the heuristic arguments break-down and underestimate the numerically observed power-law by a factor of L . This case therefore requires further study in order to correctly predict the numerically observed power-laws.

Finally, we comment on the possibility of experimental systems where our model could be realized. It seems difficult to find a material system with the hopping parameters of our model. However, with the developments in synthesizing arbitrary lattice models using degenerate cavity systems³⁶, it could be possible to realize our proposed Hamiltonian and observe its rich transport behaviors. In fact, such optical cavities have been already used to simulate 2D topological insulators, and their edge-state transport properties³⁷.

VI. ACKNOWLEDGMENTS

I thank Marko Žnidarič and Yu-Peng Wang for useful discussions. I also acknowledge support by Grant No. J1-4385 from the Slovenian Research Agency.

-
- ¹ P. W. Anderson, “Absence of diffusion in certain random lattices,” *Phys. Rev.* **109**, 1492–1505 (1958).
- ² Tōru Hirota and Kazushige Ishii, “Exactly Soluble Models of One-Dimensional Disordered Systems,” *Progress of Theoretical Physics* **45**, 1713–1715 (1971).
- ³ E. Abrahams, P. W. Anderson, D. C. Licciardello, and T. V. Ramakrishnan, “Scaling theory of localization: Absence of quantum diffusion in two dimensions,” *Phys. Rev. Lett.* **42**, 673–676 (1979).
- ⁴ Patrick A. Lee and T. V. Ramakrishnan, “Disordered electronic systems,” *Rev. Mod. Phys.* **57**, 287–337 (1985).
- ⁵ Akshay Krishna and R.N. Bhatt, “Beyond the universal dyson singularity for 1-d chains with hopping disorder,” *Annals of Physics* **435**, 168537 (2021), special Issue on Localisation 2020.
- ⁶ B. Bertini, F. Heidrich-Meisner, C. Karrasch, T. Prosen, R. Steinigeweg, and M. Žnidarič, “Finite-temperature transport in one-dimensional quantum lattice models,” *Rev. Mod. Phys.* **93**, 025003 (2021).
- ⁷ Marko Žnidarič, Antonello Scardicchio, and Vipin Kerala Varma, “Diffusive and subdiffusive spin transport in the ergodic phase of a many-body localizable system,” *Phys. Rev. Lett.* **117**, 040601 (2016).
- ⁸ Wojciech De Roeck, Francois Huveneers, and Stefano Olla, “Subdiffusion in one-dimensional hamiltonian chains with sparse interactions,” *Journal of Statistical Physics* **180**, 678–698 (2020).
- ⁹ Iliia Khait, Snir Gazit, Norman Y. Yao, and Assa Auerbach, “Spin transport of weakly disordered heisenberg chain at infinite temperature,” *Phys. Rev. B* **93**, 224205 (2016).
- ¹⁰ S. J. Thomson, “Localization and subdiffusive transport in quantum spin chains with dilute disorder,” *Phys. Rev. B* **107**, 014207 (2023).
- ¹¹ Madhumita Saha, Bijay Kumar Agarwalla, Manas Kulkarni, and Archak Purkayastha, “Universal subdiffusive behavior at band edges from transfer matrix exceptional points,” *Phys. Rev. Lett.* **130**, 187101 (2023).
- ¹² Junaid Majeed Bhat, “Topologically protected subdiffusive transport in two-dimensional fermionic wires,” *Phys. Rev. B* **109**, 125415 (2024).
- ¹³ Tamoghna Ray and Junaid Majeed Bhat, “Conductance at the band edges of 2d and 3d fermionic wires,” In preparation.
- ¹⁴ David H. Dunlap, H-L. Wu, and Philip W. Phillips, “Absence of localization in a random-dimer model,” *Phys. Rev. Lett.* **65**, 88–91 (1990).
- ¹⁵ Yu-Peng Wang, Jie Ren, and Chen Fang, “Superdiffusive transport on lattices with nodal impurities,” arXiv preprint arXiv:2404.16927 (2024).
- ¹⁶ Hisashi Hiramoto and Shuji Abe, “Dynamics of an electron in quasiperiodic systems. i. fibonacci model,” *Journal of the Physical Society of Japan* **57**, 230–240 (1988).
- ¹⁷ Marko Ljubotina, Marko Žnidarič, and Tomaž Prosen, “Spin diffusion from an inhomogeneous quench in an integrable system,” *Nature communications* **8**, 16117 (2017).
- ¹⁸ Marko Ljubotina, Marko Žnidarič, and Tomaž Prosen, “Kardar-parisi-zhang physics in the quantum heisenberg magnet,” *Phys. Rev. Lett.* **122**, 210602 (2019).
- ¹⁹ Marko Žnidarič, “Spin transport in a one-dimensional anisotropic heisenberg model,” *Phys. Rev. Lett.* **106**, 220601 (2011).
- ²⁰ Yu-Peng Wang, Chen Fang, and Jie Ren, “Superdiffusive transport in quasi-particle dephasing models,” arXiv preprint arXiv:2310.03069 (2023).
- ²¹ Hirotsugu Matsuda and Kazushige Ishii, “Localization of Normal Modes and Energy Transport in the Disordered Harmonic Chain*,” *Progress of Theoretical Physics Supplement* **45**, 56–86 (1970).
- ²² Sajeed John, “Strong localization of photons in certain disordered dielectric superlattices,” *Phys. Rev. Lett.* **58**, 2486–2489 (1987).
- ²³ Sajeed John, H. Sompolinsky, and Michael J. Stephen, “Localization in a disordered elastic medium near two dimensions,” *Phys. Rev. B* **27**, 5592–5603 (1983).
- ²⁴ A. Casher and J. L. Lebowitz, “Heat Flow in Regular and Disordered Harmonic Chains,” *Journal of Mathematical Physics* **12**, 1701–1711 (1971).
- ²⁵ Robert J. Rubin and William L. Greer, “Abnormal Lattice Thermal Conductivity of a One-Dimensional, Harmonic, Isotopically Disordered Crystal,” *Journal of Mathematical Physics* **12**, 1686–1701 (1971).
- ²⁶ Gaëtan Cane, Junaid Majeed Bhat, Abhishek Dhar, and Cédric Bernardin, “Localization effects due to a random magnetic field on heat transport in a harmonic chain,” *Journal of Statistical Mechanics: Theory and Experiment* **2021**, 113204 (2021).
- ²⁷ Theo Verheggen, “Transmission coefficient and heat conduction of a harmonic chain with random masses: asymptotic estimates on products of random matrices,” *Communications in Mathematical Physics* **68**, 69–82 (1979).
- ²⁸ Abhishek Dhar, “Heat conduction in the disordered harmonic chain revisited,” *Phys. Rev. Lett.* **86**, 5882–5885 (2001).
- ²⁹ Dibyendu Roy and Abhishek Dhar, “Role of pinning potentials in heat transport through disordered harmonic chains,” *Phys. Rev. E* **78**, 051112 (2008).
- ³⁰ Oskari Ajanki and François Huveneers, “Rigorous scaling law for the heat current in disordered harmonic chain,” *Communications in mathematical physics* **301**, 841–883 (2011).
- ³¹ Wojciech De Roeck, Abhishek Dhar, Francois Huveneers, and Marius Schütz, “Step density profiles in localized chains,” *Journal of Statistical Physics* **167**, 1143–1163 (2017).
- ³² Abhishek Dhar and Diptiman Sen, “Nonequilibrium green’s function formalism and the problem of bound

- states,” Phys. Rev. B **73**, 085119 (2006).
- ³³ Junaid Majeed Bhat and Abhishek Dhar, “Transport in spinless superconducting wires,” Phys. Rev. B **102**, 224512 (2020).
- ³⁴ Harry Furstenberg, “Noncommuting random products,” Transactions of the American Mathematical Society **108**, 377–428 (1963).
- ³⁵ Hans Crauel, Matthias Gundlach, and Volker Wihstutz, “Perturbation methods for lyapunov exponents,” Stochastic dynamics , 209–239 (1999).
- ³⁶ Su Wang, Xiang-Fa Zhou, Guang-Can Guo, Han Pu, and Zheng-Wei Zhou, “Synthesizing arbitrary lattice models using a single degenerate cavity,” Physical Review A **100**, 043817 (2019).
- ³⁷ Xi-Wang Luo, Xingxiang Zhou, Chuan-Feng Li, Jin-Shi Xu, Guang-Can Guo, and Zheng-Wei Zhou, “Quantum simulation of 2d topological physics in a 1d array of optical cavities,” Nature communications **6**, 7704 (2015).
- ³⁸ Dibyendu Roy and Abhishek Dhar, “Heat transport in ordered harmonic lattices,” Journal of Statistical Physics **131**, 535–541 (2008).

Appendix A: The Reservoir Hamiltonians

Let us label the annihilation and creation operators at a site (x, y) as $(\psi(x, y), \psi^\dagger(x, y))$, and $(\phi_{L/R}(x, y), \phi_{L/R}^\dagger(x, y))$ on the wire, the left lead and the right lead, respectively. These satisfy the usual Fermionic anti-commutation relations. Free boundary conditions are imposed at the horizontal edges of the reservoir and the system at $y = 1$ and $y = W$, respectively. The contacts between the wire and the reservoirs are themselves modeled as tight-binding Hamiltonians, \mathcal{H}_{WL} and \mathcal{H}_{WR} . To write the full Hamiltonian of system, we define column vectors $\Psi(x)$, and $\Phi_{L/R}(x)$ of W components with the y^{th} component given by the operators $\psi(x, y)$ and $\phi_{L/R}(x, y)$, respectively. Therefore, we have the following for the full Hamiltonian of the system,

$$\mathcal{H} = \mathcal{H}_L + \mathcal{H}_{LW} + \mathcal{H}_W + \mathcal{H}_{RW} + \mathcal{H}_R, \quad (\text{A1})$$

where the individual Hamiltonians of the wire, the contacts, and the reservoirs are given by,

$$\mathcal{H}_W = \sum_{x=1}^L \epsilon_x \Psi^\dagger(x) H_0 \Psi(x) + \sum_{x=1}^{L-1} [\Psi^\dagger(x) \Psi(x+1) + \text{h.c.}], \quad (\text{A2})$$

$$\mathcal{H}_{LW} = \eta_c (\Psi^\dagger(1) \Phi_L(0) + \Phi_L^\dagger(0) \Psi(1)), \quad (\text{A3})$$

$$\mathcal{H}_{RW} = \eta_c (\Psi^\dagger(L) \Phi_R(L+1) + \Phi_R^\dagger(L+1) \Psi(L)), \quad (\text{A4})$$

$$\mathcal{H}_L = \sum_{x=-\infty}^0 \Phi_L^\dagger(x) H'_0 \Phi_L(x) + \eta_{bx} \sum_{x=-\infty}^{-1} \Phi_L^\dagger(x) \Phi_L(x+1) + \Phi_L^\dagger(x+1) \Phi_L(x), \quad (\text{A5})$$

$$\mathcal{H}_R = \sum_{x=L+1}^{\infty} \Phi_R^\dagger(x) H'_0 \Phi_R(x) + \eta_{bx} \sum_{x=L+1}^{\infty} \Phi_R^\dagger(x) \Phi_R(x+1) + \Phi_R^\dagger(x+1) \Phi_R(x). \quad (\text{A6})$$

Note that we have taken the reservoir Hamiltonians to be the same and the couplings at the contacts are assumed to be of strength η_c .

Appendix B: Simplification of NEGF Conductance

The NEGF formula for conductance for arbitrary lattice models is given by,

$$T(E) = 4\pi^2 \text{Tr}[G^+(E) \Gamma_L(E) G^-(E) \Gamma_R(E)], \quad (\text{B1})$$

where $G^+(E) = (E - H_W - \Sigma_L(E) - \Sigma_R(E))^{-1}$ is the effective Green’s function of the wire and $\Gamma_{L/R} = (\Sigma_{L/R}^\dagger - \Sigma_{L/R})/(2\pi i)$. Since the contacts with the reservoirs are only along the edges i.e. at $x = 1$, and $x = L$, the trace in Eq. (B1) can be computed as,

$$T(E) = 4\pi^2 \text{Tr}[G_{1L}^+ \Gamma G_{L1}^- \Gamma], \quad (\text{B2})$$

where G_{1L}^+ is a $W \times W$ matrix with components given by, $G_{1L}^+[y, y'] = G^+(E)[x = 1, y; x' = L, y']$ and $G_{L1}^- = [G_{1L}^+]^\dagger$. Γ is the only non-zero block of $\Gamma_{L/R}$ given by, $\Gamma[y, y'] = \Gamma_R[L, y; L, y'] = \Gamma_L[1, y; 1, y']$.

Using the transfer matrix approach, it can be shown that¹²,

$$\tilde{G}_{1L}^+ = [P_L + \tilde{\Sigma} P_{L-1} + Q_L \tilde{\Sigma} + \tilde{\Sigma} Q_{L-1} \tilde{\Sigma}]^{-1} \quad (\text{B3})$$

The tilde over the Green function and self energy matrices denotes that these are written in the diagonal basis of H_0 i.e. $\tilde{G}_{1L}^+[y, y'] = -U G_{1L}^+ U^\dagger$. Similarly, $\tilde{\Sigma}[y, y'] = U \Sigma[y, y'] U^\dagger = U \Sigma_R[L, y; L, y'] U^\dagger = U \Sigma_L[1, y; 1, y'] U^\dagger$, is the only non-zero block of the matrices Σ_L and Σ_R . P_L and Q_L are diagonal matrices with entries given by $p_L(\lambda_k)$ and $q_L(\lambda_k)$, $k = 1, 2, 3, \dots, W$, which are defined in the main text.

It can be shown that $\Sigma = U_L \Sigma_D U_L^\dagger$, where Σ_D is a diagonal matrix with components given by³²,

$$\Sigma_D[k, k] = \begin{cases} \frac{\eta_c^2}{\eta_{bx}^2} [z_k + i\sqrt{1-z_k^2}]; & |z_k| < 1, \\ \frac{\eta_c^2}{\eta_{bx}^2} [z_k - \sqrt{z_k^2-1}]; & z_k > 1, \\ \frac{\eta_c^2}{\eta_{bx}^2} [z_k + \sqrt{z_k^2-1}]; & z_k < -1, \end{cases} \quad (\text{B4})$$

where $z_k = \frac{E-\lambda'_k}{2\eta_{bx}}$. U_L is the unitary transformation that diagonalizes the intra-chain hopping matrix H'_0 of the reservoirs and its eigenvalues are given by λ'_k . We consider the limit where $|\eta_{bx}| \gg |\omega - \tilde{\lambda}_k|$ for all k . Note that if H'_0 is chosen to correspond to nearest-neighbor hopping model with hopping η_{by} , then $\lambda'_k = 2\eta_{by} \cos[\frac{k\pi}{W+1}]$ and the limiting condition reads $|\eta_{bx}| \gg |E| + 2|\eta_{by}|$. In this limit, $\tilde{\Sigma} \approx \Sigma \approx \Sigma_D \approx i\gamma I$ and $\Gamma \approx \frac{\gamma}{\pi} I$, where $\gamma = \eta_c^2/\eta_{bx}$. Thus, Eq. (B2) reduces to,

$$T(E) \approx 4 \sum_{k=1}^W \frac{\gamma^2}{|p_L(\lambda_k) + i\gamma[p_{L-1}(\lambda_k) + q_L(\lambda_k)] - \gamma^2 q_{L-1}(\lambda_k)|^2} \quad (\text{B5})$$

$$= 4 \sum_{k=1}^W |F_L(\lambda_k)|^2. \quad (\text{B6})$$

The sum over k in Eq. (B6) sums over the eigenvalues of H_0 and in the limit $W \rightarrow \infty$, this sum can be replaced by an integral over the spectrum of H_0 given by $\mu + 2\cos(\mathbf{k})$, $\mathbf{k} \in (0, \pi)$,

$$\tau(E) = \frac{T(E)}{W} \approx \frac{4}{\pi} \int_0^\pi d\mathbf{k} |F_L(\lambda_{\mathbf{k}})|^2, \quad (\text{B7})$$

where $\tau(E)$ is the conductance per unit width of the wire.

Appendix C: Lyapunov Exponent Proof

We begin rewriting Eq. (9) as,

$$\zeta(\lambda) = \int_{-\pi/2}^{\pi/2} d\theta \mathbf{P}[\theta, \lambda] \log \left| \frac{\cos(\theta + h(\lambda, E))}{\cos \theta} \right| \quad (\text{C1})$$

$$= \int_{-\pi/2}^{\pi/2} d\theta (\mathbf{P}[\theta - h(\lambda), \lambda] - \mathbf{P}[\theta, \lambda]) \log |\cos \theta| \quad (\text{C2})$$

We have used the fact that $\mathbf{P}[\theta, \lambda]$ is periodic as the iteration equation, Eq. (7), is itself periodic in the variable θ . We Taylor expand Eq. (C2) around $\lambda = 0$, to obtain the coefficients $\zeta_0(\theta, E)$, $\zeta_1(\theta, E)$ and $\zeta_2(\theta, E)$ as,

$$\zeta_0(\theta, E) = \mathbf{P}_0(\theta - h_0(E)) - \mathbf{P}_0(\theta) \quad (\text{C3})$$

$$\zeta_1(\theta, E) = -h_1(E) \partial_\theta \mathbf{P}_0(\theta - h_0(E)) + \mathbf{P}_1(\theta - h_0(E)) - \mathbf{P}_1(\theta) \quad (\text{C4})$$

$$\zeta_2(\theta, E) = -h_2(E) \partial_\theta \mathbf{P}_0(\theta - h_0(E)) + \frac{h_1(E)^2}{2} \partial_\theta^2 \mathbf{P}_0(\theta - h_0(E)) - h_1(E) \partial_\theta \mathbf{P}_1(\theta - h_0(E)) + \mathbf{P}_2(\theta - h_0(E)) - \mathbf{P}_2(\theta). \quad (\text{C5})$$

Let us now Taylor expand the self consistency equation of $\mathbf{P}[\theta, \lambda]$, Eq. (11). For the zeroth, first and second order we have,

$$\mathbf{P}_0(\theta) - \mathbf{P}_0(\theta - h_0(E)) = 0, \quad (\text{C6})$$

$$\mathbf{P}_1(\theta) - \left[\partial_\theta \mathbf{P}_0(\theta - h_0(E)) \langle \Theta_1 \rangle + \mathbf{P}_1(\theta - h_0(E)) + \partial_\theta \langle \Theta_1 \rangle \mathbf{P}_0(\theta - h_0(E)) \right] = 0, \quad (\text{C7})$$

$$\begin{aligned} \mathbf{P}_2(\theta) - \left[\mathbf{P}_2(\theta - h_0(E)) + \partial_\theta \mathbf{P}_0(\theta - h_0(E)) \langle \Theta_2 \rangle + \frac{1}{2} \partial_\theta^2 \mathbf{P}_0(\theta - h_0(E)) \langle \Theta_1^2 \rangle + \partial_\theta \mathbf{P}_1(\theta - h_0(E)) \langle \Theta_1 \rangle \right. \\ \left. + \mathbf{P}_0(\theta - h_0(E)) \partial_\theta \langle \Theta_2 \rangle + (\partial_\theta \mathbf{P}_0(\theta - h_0(E)) \langle \Theta_1 \rangle + \mathbf{P}_1(\theta - h_0(E)) \partial_\theta \langle \Theta_1 \rangle) \right] = 0, \end{aligned} \quad (\text{C8})$$

where we assumed $\Theta[\theta, \lambda] = \theta - h_0(E) + \sum_{i=1}^\infty \Theta_i(\theta) \lambda^i$.

Eq. (C6) immediately gives $\zeta_0(\theta, E) = 0$. To show that $\zeta_1(\theta, E) = 0$, we consider the expansion of functions $\langle \Theta[\theta, \lambda] \rangle$ and $h(\lambda, E)$ around $\lambda = 0$,

$$h(\lambda) = h_0(E) - \frac{\langle \epsilon \rangle \lambda}{(4 - E^2)^{1/2}} + \frac{E \langle \epsilon \rangle^2 \lambda^2}{2(4 - E^2)^{3/2}} + \mathcal{O}(\lambda^3) \quad (\text{C9})$$

$$\begin{aligned} \langle \Theta[\theta, \lambda] \rangle &= \theta - h_0(E) + \frac{\langle \epsilon \rangle \lambda}{(4 - E^2)^{1/2}} \\ &- \left[\frac{E \langle \epsilon \rangle^2 + 8\sqrt{4 - E^2} \sigma^2 \cos^3 \theta \sin \theta}{2(4 - E^2)^{3/2}} \right] \lambda^2 + \mathcal{O}(\lambda^3) \end{aligned} \quad (\text{C10})$$

where $\sigma^2 = \langle (\epsilon_x - \langle \epsilon \rangle)^2 \rangle$ and $h_0(E) = \arccos[-E/2]$. Note that $\langle \Theta_1 \rangle = -h_1(E)$ and $\partial_\theta \langle \Theta_1 \rangle = 0$. Using these

two in Eq. (C7) we get,

$$\mathbf{P}_1(\theta) + h_1(E)\partial_\theta\mathbf{P}_0(\theta - h_0(E)) - \mathbf{P}_1(\theta - h_0(E)) = 0 \quad (\text{C11})$$

and therefore $\zeta_1(\theta, E) = 0$. Let us now compute ζ_2 , for this note that Eq. (C6) implies that $\mathbf{P}_0(\theta)$ is a constant, as the equation holds for arbitrary $|E| < 2$. Fixing $\mathbf{P}_0(\theta)$ using normalization to $\frac{1}{\pi}$, and substituting in Eq. (C5) and Eq. (C8) we get,

$$\begin{aligned} \zeta_2(\theta, E) = & -h_1(E)\partial_\theta\mathbf{P}_1(\theta - h_0(E)) \\ & + \mathbf{P}_2(\theta - h_0(E)) - \mathbf{P}_2(\theta), \end{aligned} \quad (\text{C12})$$

$$- \mathbf{P}_2(\theta) + \mathbf{P}_2(\theta - h_0(E)) - h_1(E)\partial_\theta\mathbf{P}_1(\theta - h_0(E)) + \frac{1}{\pi}\partial_\theta\langle\Theta_2\rangle = 0 \quad (\text{C13})$$

Comparing these two equations, we get $\zeta_2(\theta, E) = -\frac{1}{\pi}\partial_\theta\langle\Theta_2\rangle$ where Θ_2 is given by Eq. (C10). Therefore, the Lyapunov exponent is given by,

$$\zeta(\lambda) = -\frac{\lambda^2}{\pi} \int_{-\pi/2}^{\pi/2} d\theta \log |\cos \theta| \partial_\theta \langle\Theta_2\rangle + \mathcal{O}(\lambda^3) \quad (\text{C14})$$

$$= \frac{\sigma^2}{2(4 - E^2)} \lambda^2 + \mathcal{O}(\lambda^3). \quad (\text{C15})$$

Note that the pre-factor of λ^2 is positive only in the domain of the applicability of the solution, $|E| < 2$. At $|E| = 2$ it diverges, reminiscent of the fact that at this point the behavior is different.

Appendix D: Derivation of $\bar{F}^o(q_{\mathbf{k}})$

If $\epsilon_x = \langle\epsilon\rangle$ for all x , then it is straightforward to see that $p_L(\lambda_{\mathbf{k}}) = \sin[q_{\mathbf{k}}(L+1)]/\sin[q_{\mathbf{k}}]$, which gives

$$F_L^o(\lambda_{\mathbf{k}}) = \frac{\gamma \sin q_{\mathbf{k}}}{\sin q_{\mathbf{k}}(L+1) + 2i\gamma \sin q_{\mathbf{k}}L - \gamma^2 \sin q_{\mathbf{k}}(L-1)}. \quad (\text{D1})$$

We rewrite this expression for $F_L^o(\lambda_{\mathbf{k}})$ as follows,

$$F_L^o(\lambda_{\mathbf{k}}) = \frac{\gamma \sin q_{\mathbf{k}}}{A(q_{\mathbf{k}}) \sin Lq_{\mathbf{k}} + B(q_{\mathbf{k}}) \sin q_{\mathbf{k}} \cos Lq_{\mathbf{k}}}, \quad (\text{D2})$$

where $A(q_{\mathbf{k}}) = (1 - \gamma^2) \cos q_{\mathbf{k}} + 2i\gamma$ and $B(q_{\mathbf{k}}) = (1 + \gamma^2)$. Therefore, for a disorder free chain we have,

$$\tau_0(E) = \frac{4\gamma^2}{\pi} \int_0^\pi d\mathbf{k} \frac{\sin^2 q_{\mathbf{k}}}{|A(q_{\mathbf{k}}) \sin Lq_{\mathbf{k}} + B(q_{\mathbf{k}}) \sin q_{\mathbf{k}} \cos Lq_{\mathbf{k}}|^2} \quad (\text{D3})$$

$$= \frac{8\gamma^2}{\pi} \int_0^\pi d\mathbf{k} \sin^2 q_{\mathbf{k}} \frac{[|A(q_{\mathbf{k}})|^2 + |B(q_{\mathbf{k}})|^2 \sin^2 q_{\mathbf{k}}]^{-1}}{1 + R(q_{\mathbf{k}}) \sin[2Lq_{\mathbf{k}} + \theta(q_{\mathbf{k}})]} \quad (\text{D4})$$

$$\approx \frac{8\gamma^2}{\pi} \int_0^\pi dq \left| \frac{d\mathbf{k}}{dq} \right| \sin^2 q \frac{[|A(q)|^2 + |B(q)|^2 \sin^2 q]^{-1}}{1 + R(q) \sin[2Lq + \theta(q)]}, \quad (\text{D5})$$

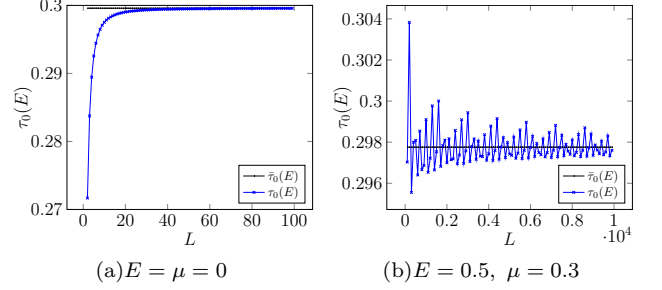


FIG. 4. Convergence of $\tau_0(E)$ to $\bar{\tau}_0(E)$. Parameter values: $W = 10^4$, $\langle\epsilon\rangle = 1$, and $\gamma = 0.25$.

where, $R(q_{\mathbf{k}})$ and $\theta(q_{\mathbf{k}})$ are defined via the relations,

$$R(q_{\mathbf{k}}) \cos[\theta(q_{\mathbf{k}})] = \frac{2 \operatorname{Re}[A(q_{\mathbf{k}})B^*(q_{\mathbf{k}})] \sin q_{\mathbf{k}}}{|A(q_{\mathbf{k}})|^2 + |B(q_{\mathbf{k}}) \sin q_{\mathbf{k}}|^2}, \quad (\text{D6})$$

$$R(q_{\mathbf{k}}) \sin[\theta(q_{\mathbf{k}})] = \frac{|A(q_{\mathbf{k}})|^2 - |B(q_{\mathbf{k}}) \sin q_{\mathbf{k}}|^2}{|A(q_{\mathbf{k}})|^2 + |B(q_{\mathbf{k}}) \sin q_{\mathbf{k}}|^2}. \quad (\text{D7})$$

Note while changing the integration variable from \mathbf{k} to $q_{\mathbf{k}}$, we kept the limits of the integration same. This approximation loses some irrelevant details of $\tau_0(E)$ but helps to take the limit $L \rightarrow \infty$. We will discuss what details are lost when we present some numerical results by the end of this section. In the limit $L \rightarrow \infty$, we have,

$$\bar{\tau}_0(E) = \frac{8\gamma^2}{\pi} \lim_{L \rightarrow \infty} \int_0^\pi dq \left| \frac{d\mathbf{k}}{dq} \right| \frac{\sin^2 q}{|1 + R(q) \sin[2Lq + \theta(q)]|} \quad (\text{D8})$$

$$= \frac{8\gamma^2}{\pi} \int_0^\pi dq \left| \frac{d\mathbf{k}}{dq} \right| \frac{\sin^2 q}{\sqrt{1 - R^2(q)}}, \quad (\text{D9})$$

where the last step follows from the identity³⁸,

$$\lim_{N \rightarrow \infty} \int_0^\pi du \frac{g(u)}{1 + h(u) \sin[2uN + r(u)]} = \int_0^\pi du \frac{g(u)}{\sqrt{1 - h^2(u)}}. \quad (\text{D10})$$

Converting the integral in Eq. (D9) back from q to k and then substituting $\frac{1}{\sqrt{1 - R^2(q_{\mathbf{k}})}} = \frac{|A(q_{\mathbf{k}})|^2 + |B(q_{\mathbf{k}}) \sin q_{\mathbf{k}}|^2}{2 \operatorname{Im}[A(q_{\mathbf{k}})B^*(q_{\mathbf{k}})] \sin q_{\mathbf{k}}}$ we have,

$$\bar{\tau}_0(E) = \frac{8\gamma^2}{\pi} \int_0^\pi d\mathbf{k} \frac{\sin q_{\mathbf{k}}}{2 \operatorname{Im}[A(q_{\mathbf{k}})B^*(q_{\mathbf{k}})]} \quad (\text{D11})$$

$$= \frac{4}{\pi} \int_0^\pi d\mathbf{k} \bar{F}^o(q_{\mathbf{k}}). \quad (\text{D12})$$

We show in Fig. (4) the convergence of $\tau_0(E)$ to $\bar{\tau}_0(E)$ as L is increased. Note that Fig. (4a), the parameters are such that $q_{\mathbf{k}} = \mathbf{k}$, so the change of limits from Eq. (D4) to Eq. (D5) is exact and we see a smooth convergence to the expected value from the theory. When the parameter values are such that the change of limits is not exact Fig. (4b), we see highly oscillating behavior around

the theoretically expected value in the numerical calculation. Though the oscillations are not captured by the

approximation, they are irrelevant for the scaling of the conductance.